

COVER SHEET

*NOTE: This coversheet is intended for you to list your article title and author(s) name only
—this page will not appear on the Electronic Product.*

**Title: Stiffness and Fatigue Life Estimator for Polymer Composite Laminates
Using Machine Learning**

Authors: Steven M. Arnold
Subodh K. Mital
Brandon L. Hearley

PAPER DEADLINE: ****June 9, 2023****

PAPER LENGTH: ****6-16 PAGES** (Maximum – not counting cover page) ******

SUBMISSION PROCEDURE: **Information on the electronic submission of
manuscripts is provided on the conference web site:**

<https://www.asc-composites.org/content.asp?contentid=207>

Paper Number: **004673**

FILE NAME: 004673_Arnold.doc

**We encourage you to read attached Guidelines prior to preparing your paper—this will ensure
your paper is consistent with the format of the articles in the Electronic product.**

NOTE: Please submit your paper in Microsoft Word® format or PDF if prepared in a program other than MSWord. Sample guidelines are shown with the correct margins. Follow the style from these guidelines for your page format.

Electronic file submission: When making your final PDF for submission make sure the box at “Printed Optimized PDF” is checked. Also—in Distiller—make certain all fonts are embedded in the document before making the final PDF.

NOTES:

- Use this document file as a template to prepare your paper
- 1st page will be the Cover Page
- Do not include page numbers
- File size should not be greater than 10 Mb; resize/compress images as needed.

ABSTRACT

Machine learning (ML) models are increasingly being used in many engineering fields due to the advancements in ML algorithms and availability of high-speed computing power. One of the most popular ML class of models is artificial neural networks (ANN). ML is increasingly being used in the design and analysis of composite materials and structures, specifically in the constitutive modeling of composite materials with the focus on greatly accelerating multiscale analyses of composite materials and structures through development of surrogate models. Towards that end, Python-based neural nets have been developed to predict initial stiffness and fatigue life of an eight-ply symmetric polymer matrix composite laminate. Two types of neural networks, a Multilayer Perceptron (MLP) and a Recurrent Neural Network (RNN), have been established. Results show that both neural net type algorithms can provide an excellent estimate of initial laminate stiffness as well as fatigue life of eight-ply symmetric polymer matrix composite laminates (PMCs). RNNs are better able to capture the shape of the fatigue curve of a laminate. The resulting tool and GUI can be very useful for system level studies to obtain an estimate of desired properties and life of PMC composite laminates. Further, the associated surrogate models can also be used in composite multiscale analyses to replace the actual physics-based calculations at lower scales and thereby significantly increase the computational efficiency of such analyses and thus make micromechanics-based multiscale analyses a viable industrial tool for large scale structural problems.

INTRODUCTION

In recent years, the phraseology artificial intelligence (AI), machine learning (ML) and deep learning artificial neural network (ANN) appear in countless articles with a promise of achieving self-driving cars, intelligent chatbots, and virtual assistants etc. [1]. ANN are a subset of ML, which itself is a subset of AI. AI can be thought of as a process that tries to automate intellectual tasks that are normally expected to be performed by humans. As mentioned, AI is much more than ML. Previously, research was done in symbolic AI, which does not involve any learning. Researchers believed that by programming a sufficiently large number of explicit rules, human level intelligence could be achieved [2]. Such an approach seemed to work to solve logical problems such as playing chess; however, it proved insufficient in solving complex problems such as image classification, speech recognition, language translation etc. which resulted in developing new approaches now known as ML. Today, machine learning is being employed in a wide range of computing tasks where designing and programming explicit algorithms is infeasible [3].

Deep learning, mentioned in relation to ML, refers to systems with more than one layer of neurons between the input and output layers and associated weights applied to each neuron. It has been observed that multi-layer networks can learn and interpret relations that single layer networks cannot learn. The elements of a neural network are nodes or neurons, where weighted signals are combined, and biases added. In a single layer, the inputs are multiplied by weights and then added with a bias, before passing through a non-linear activation function. In a multi-layer or “deep learning” network, the inputs are combined in the second layer before being output [4]. It is highly linked to optimization techniques as it’s trying to find the most optimum weights for each node that will minimize the error between the prediction and the target result. Figure 1 shows the anatomy of a deep learning neural network.

Another fast-growing discipline with emphasis on reducing the cost and time to market of new materials is Integrated Computational Materials Engineering (ICME). ICME is an integrated approach to the design of products and the materials which comprise them by linking multiple models at different time and length scales [5,6]. At present, such analyses that link atomistic scale models to structural scale models are extremely resource intensive, often requiring the use of high-performance computing platforms. If some of these analyses at some scales could be replaced by artificial neural nets through surrogate modeling, it has the potential to greatly enhance the computational efficiency without sacrificing the accuracy required.

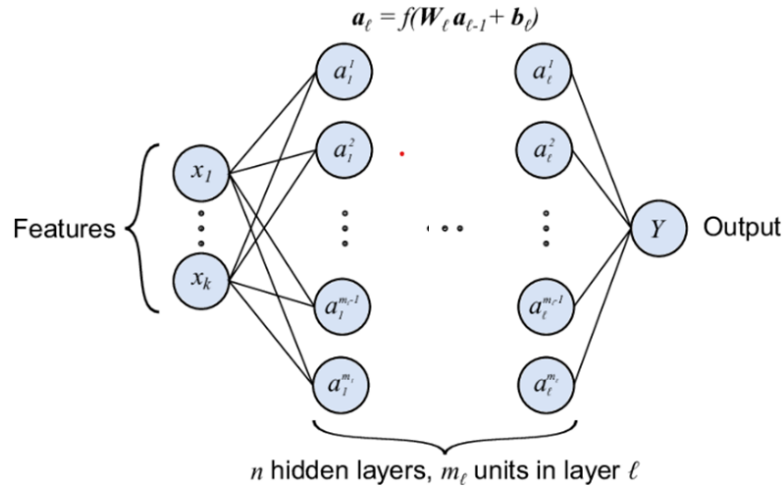


Figure 1. Anatomy of a deep learning neural network

ML is increasingly being used in the design and analysis of composite materials and structures, specifically in the constitutive modeling of composite materials with the focus on greatly accelerating multiscale analyses of composite materials and structures [7,8,9]. Towards that end, our objective is to provide designers a Python-based ML surrogate model, that can rapidly predict the initial stiffness (ABD matrices) and fatigue lives (S-N Curve) of polymer matrix composite (PMC) laminates. Since ML models typically require large amounts of data for training and validation and this quantity of measured data is not readily available, synthetic (virtual/simulated) data is generated using NASA's MAC/GMC (Micromechanics Analysis Code using Generalized Method of Cells) computer code [10]. MAC/GMC is a comprehensive, physics-based, composite material and laminate analysis tool that utilizes the method of cells family (MOC, GMC and HFGMC) of micromechanics theories [11,12]. The current ML model has focused on predicting initial laminate stiffnesses and fatigue life of thermoelastic eight-ply, symmetric, PMC laminates subjected to stiffness reduction progressive cyclic damage. Results show that the trained surrogate ML model provides reasonable estimates of the desired composite behavior for a fraction (10^{-4}) of the computational cost of the corresponding physics-based model. Consequently, such an approach will lead to efficient, robust, and accurate data-driven design and analysis of composite materials and structures.

OVERVIEW OF MAC/GMC COMPUTER CODE

The Generalized Method of Cells (GMC), first developed by Paley and Aboudi [13] and the High Fidelity Generalized Method of Cells (HFGMC), first developed by Aboudi et al. [14], are semi-analytical in nature, and their formulation involves application of several governing conditions (e.g., traction and displacement compatibility) in an average sense within a repeating unit cell (RUC). They provide the local fields in composite materials, allowing incorporation of arbitrary inelastic constitutive models with various deformation and damage constitutive laws. The microstructure of a periodic multiphase material, within the context of GMC and HFGMC, is represented by a doubly periodic (continuously reinforced) or triply periodic (discontinuously reinforced) RUC consisting of an arbitrary number of subcells, each of which may be a distinct material (Figure 2). In the case of GMC, the displacement field is assumed

linear, whereas in the case of HFGMC the displacement approximations are assumed quadratic, thus leading to a constant and linear subcell strain field, respectively. In fact, it is precisely this higher order assumption in the displacement field that enables HFGMC to retain its ability to compute nonzero transverse shear stress distributions within the composite (i.e., normal and shear coupling) when global tensile loading is applied. This shear coupling is very important when dealing with disordered microstructures [15,16]. However, it is also this high-order field assumption which makes HFGMC more computationally expensive and subject to subcell discretization dependence as compared to GMC.

Displacement and traction continuity are enforced in an average, or integral, sense at each of the subcell interfaces and the periodic boundaries of the RUC. These continuity conditions are used to formulate a strain concentration matrix \mathbf{A} , which gives all the local subcell strains (ϵ_S) in terms of the global, average, applied strains $\epsilon_{applied}$ (i.e., $\epsilon_S = \mathbf{A} \epsilon_{applied}$). The local subcell stresses (σ) can then be calculated using the local constitutive law and the local subcell strains. Finally, the overall RUC stiffness is obtained utilizing the local constitutive law and the strain concentration matrix averaged over the RUC dimensions. The detailed methodology of GMC and HFGMC and the formulation to be embedded within classical laminate theory are described thoroughly in Aboudi et al. [11,12]. Also, in these references the superior accuracy of HFGMC over that of GMC is demonstrated, consequently in this study HFGMC will be assumed to provide the most accurate predictions.

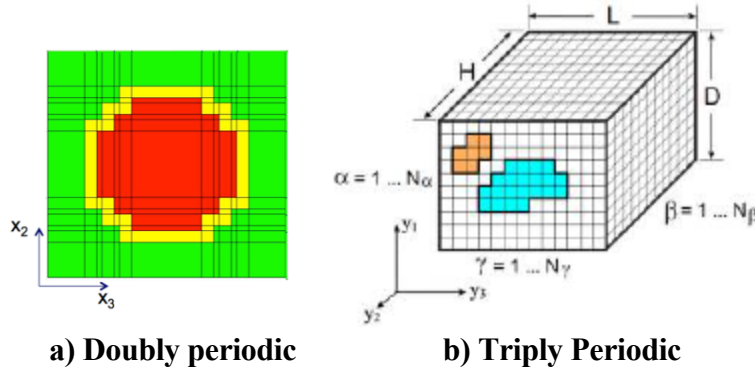


Figure 2. Composite with repeating microstructure and arbitrary constituents

Constitutive Models

The most well-known and widely used constitutive model, Hooke's law, is written as

$$\sigma_{ij} = C_{ijkl} \epsilon_{kl} \quad (1)$$

which describes time-independent, linear (proportional) reversible material behavior, where C_{ijkl} is the classic stiffness tensor and ϵ_{kl} is the elastic component of the strain tensor. Extension into the irreversible regime has been accomplished by assuming an additive decomposition of the total strain tensor into three components, that is a reversible mechanical strain (i.e., elastic/viscoelastic) ϵ_{ij} ; an irreversible (i.e., inelastic or viscoplastic) strain ϵ_{ij}^I ; and a reversible thermal strain, ϵ_{ij}^{th} component.

$$\epsilon_{ij}^{total} = \epsilon_{ij} + \epsilon_{ij}^I + \epsilon_{ij}^{th} \quad (2)$$

or

$$\epsilon_{ij} = \epsilon_{ij}^{total} - \epsilon_{ij}^I - \epsilon_{ij}^{th} \quad (3)$$

After substituting expression (3) into equation (1) we arrive at a stress strain relation (generalized Hooke's law) that incorporates irreversible strains as well as reversible ones, that is:

$$\sigma_{ij} = C_{ijkl}(\varepsilon_{kl} - \varepsilon_{kl}^I - \varepsilon_{kl}^{th}) \quad (4)$$

where numerous models describing the evolution of the inelastic strain have been proposed in the literature [17-19]. Herein we will confine this initial study to elastic constituent materials only.

Continuum Fatigue Damage Model

The fatigue life of the composite will be predicted utilizing micromechanics and the multiaxial, isothermal, continuum damage mechanics model of Arnold and Kruch [20] for the matrix constituent. When reduced to its isotropic form (i.e., parameters ω_u , ω_{fl} , ω_m , η_u , η_{fl} , and η_m are all set equal to one) this model reduces to the Non-Linear Cumulative Damage Rule (NLCDR) developed at ONERA [21]. This model assumes a single scalar internal damage variable, D , that has a value of zero for undamaged material and one for a completely damaged (or failed) material. The implementation of the damage model within GMC and HFGMC has been performed on the local scale, thus damage evolves in each subcell based on its local stress state and number of cycles. For a given damage level, the *stiffness of the subcell* is degraded by $(1 - D)$. Further, the implementation allows the application of a local damage increment ΔD , and then calculates the number of cycles, N , required to achieve this local increment of damage. This approach allows the model to determine the stress state in the composite, identify the controlling subcell that will reach the desired damage level in the fewest cycles, apply that number of cycles to all subcells, and calculate the damage that arises throughout the remainder of the composite. Then the composite can be reanalyzed, and a new stress state determined based on the new, spatially varying, damage level throughout the composite RUC. In this way, the local and global stress and damage analyses are coupled. As the damage in the composite evolves, the stress field in the composite is redistributed, which then affects the evolution of damage.

For an isotropic material, the damage parameters that must be selected reduce to M , β and a , while the pertinent equation relating the fatigue life of the isotropic material to the cyclic stress state is,

$$N_F = \frac{(\sigma_u - \sigma_{\max}) \left(\frac{M}{\sigma_{\max} - \bar{\sigma}} \right)^\beta}{\hat{a}(1 + \beta)(\sigma_{\max} - \bar{\sigma} - \sigma_{fl})} \quad \text{for } N_F > 0 \quad (5)$$

where σ_u is the material ultimate strength, σ_{fl} is the material fatigue limit (stress below which damage does not occur), σ_{\max} is the maximum stress during a loading cycle, $\bar{\sigma}$ is the mean stress during a loading cycle, and N_F is the number of cycles to failure. Note that, in the terminology of Arnold and Kruch [20], $\hat{a} = a \frac{\sigma_{fl}}{\sigma_u}$. Utilizing equation (5), the damage model parameters M , β and 'a' can be selected for an isotropic material based on the material's S-N curve (stress level vs. cycles to failure). Both the fatigue limit and the scaling parameter M are general enough to account for the effect of mean stress. However, in this study this additional effect is ignored since only one R ratio ($R = -1$, fully reversed) is examined. A representative S-N curve for an epoxy matrix was obtained, and the corresponding fatigue damage model parameters were found to be M

= 150 MPa, $\beta = 9$, and $a = 0.05$, with $\sigma_u = 80$ MPa, and $\sigma_{fl} = 27.0$ MPa. A plot showing the resulting matrix S-N curve is given in Figure 3.

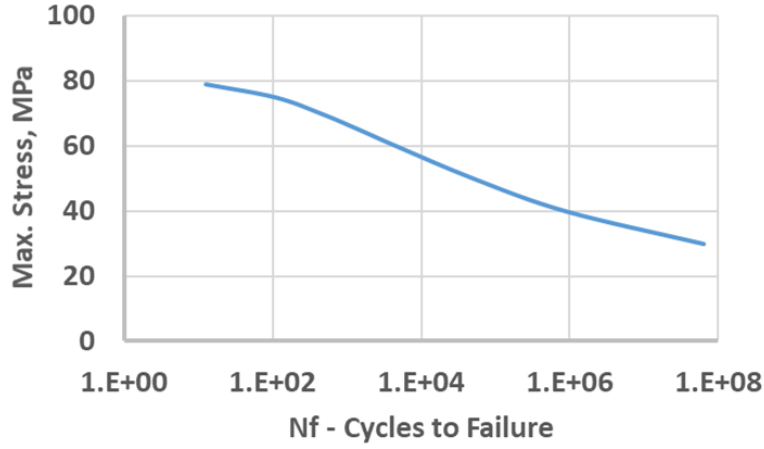


Figure 3 — *Stiffness reduction* fatigue damage model representation for epoxy matrix.

A second damage model within GMC and HFGMC is much simpler and involves degradation of a material's strength due to cyclic loading. As shown by Wilt et al. [22], this type of damage model can be used to simulate the fatigue behavior of fibers that occurs in-situ during fatigue of a composite. The model assumes a logarithmic relation between the material's strength and the number of cycles within a certain range such that:

$$\begin{aligned}
 \sigma_u &= \sigma_{u1} & 0 \leq N \leq N_1 \\
 \sigma_u &= \sigma_{u1} - \frac{(\sigma_{u1} - \sigma_{u2}) \log(N/N_1)}{\log(N_2/N_1)} & N_1 \leq N \leq N_2 \\
 \sigma_u &= \sigma_{u2} & N_2 \leq N
 \end{aligned} \tag{6}$$

This *strength degradation* model (Eq. 6) was employed in the present example to model the longitudinal fatigue behavior of the graphite fiber. The necessary parameters for the model are σ_{u1} , σ_{u2} , N_1 , and N_2 , see Example 5d in [23]. The values of these parameters chosen for a graphite fiber are shown in Fig. 4. Note that these data were not correlated with experiment, but rather chosen based on the expected trend. Given these required parameters for the fatigue damage models for each phase in the PMC, macroscopic or composite fatigue life of both unidirectional and laminate composites can be simulated. Note although creep-fatigue interaction can be incorporated in the above theory, see [24], it is not included in the present calculations.

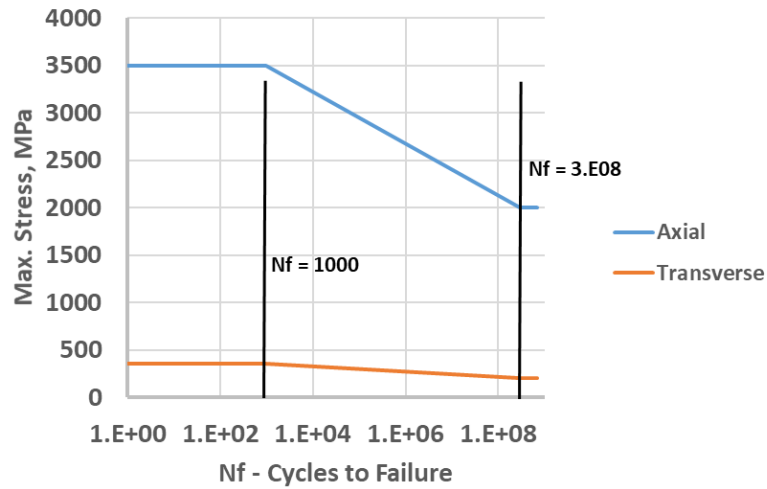


Figure 4. Strength reduction fatigue model parameters assumed for the graphite fiber.

NEURAL NETWORKS

There are different types of deep learning neural networks that have applications in different areas [25]. In general, they work well with large amounts of data and have multiple layers to learn the input/output relationships accurately. Generally, the anatomy of a neural network can be described by the following objects – (a). Layers, which are combined into a network, each containing a distinct number of neurons, (b) Input data and the corresponding targets, which is divided into training, validation, and test sets, (c) the loss function, which defines the feedback signal used for training, most common being mean-squared error (MSE), and (d) Optimizer, which determines how learning proceeds and finds the most optimal weights for each neuron that will minimize the error.

Although there are many types of neural nets [26], two types of deep learning neural nets have been investigated here – first is a Multi-layer Neural Network, also referred to as Multi-layer Perceptron (MLP) architecture and the second is a Recurrent Neural Network (RNN). MLP is the most common and basic deep learning neural network that consists of input neurons, multiple layers of hidden neurons, and output neurons. They are a fully connected feed-forward artificial neural network, sometimes loosely referred to as simply ANN. The other RNN is a type of recursive neural network which work on structured data (or data that has some functional relationship) and generally have time as the structuring element. RNN have a loop within that combines the previous time step's data with the hidden or intermediate layer to represent the current time step. They can be useful in modeling sequences of data to predict things such as future earthquakes and stock market performance and are very useful in language translation, speech recognition and many other applications. In our case, for fatigue life prediction (S-N curve) of polymer matrix composites, time is not the sequential element. Even though each stress-life pair are independent from each other yet are totally dependent upon the specific laminate defined, thus they exhibit a functional relationship between each point. Consequently, an RNN can potentially be useful in predicting the fatigue life curve (i.e., S-N curve) as it is a series of stress – life data, and thus it is a sequential series data.

DESCRIPTION OF PMC LAMINATES AND DATA GENERATION

Neural nets inherently require a significant amount of training data depending upon the number of inputs and outputs. Typically, in material science the amount of experimental data available doesn't exist in sufficient quantity due to the expense involved in generating this data. Consequently, in this study, the physics-based GMC micromechanics method was used to generate the large amount of synthetic training data. HFGMC micromechanics (a more accurate but significantly more computationally expensive, by 2-3 orders of magnitude, compared with GMC) was used to generate synthetic data as well. It was observed that for most laminates considered, there was no significant difference between GMC and HFGMC predictions particularly for fatigue lives. Stiffness matrices $[A]$ and $[D]$ ($[B] = 0$ for symmetric laminates) and fatigue lives (S-N curve) were generated for eight-ply, symmetric, regular¹ PMC laminates with varying fiber volume fractions as well as varying constituents (fiber and matrix) material properties. A 7x7 RUC, which is available within the MAC/GMC's internal library of repeating unit cells [10], was used to represent the microstructure of the composite as shown in Figure 5. Fatigue lives were predicted under a fully reversible cyclic uniaxial load applied in the global X direction. Fiber volume fractions and constituent material properties were randomly generated between some pre-defined ranges and following all applicable laws of material behavior (see Table 1, first two columns for the limits used). Twelve input values consisting of ply angles, fiber volume ratio, fiber and matrix stiffness-related properties are needed to predict the $[A]$ and $[D]$ matrices for the resulting laminate. To predict fatigue life, 7 additional fiber and matrix fatigue parameters (see Table 1) are required, as well as N_1 , N_2 , and 'a' (which were held constant at 1000, 10^9 , and 0.5 respectively) in running the MAC/GMC computer code. Note a reduction in the number of input parameters from 26 (5 for RUC/laminate, 5 for fiber elastic, 2 for matrix elastic, 8 for fiber fatigue, 6 for matrix fatigue) to 19 was achieved by assuming that the fiber strength parameters are related to each other via a Von Mises relationship (i.e., $\sqrt{3}$), see Table II. In the development of surrogate model(s), various neural net methods contained within the Python scripting environment [27] were considered. Note it is also essential that an informatics infrastructure be utilized to store not only the data (albeit virtual or real) but also more importantly the meta data for both data and ML model(s) to maximize traceability and minimize misuse, see [28]. Finally, the applied load is also required.

The stress versus cycles fatigue curve (i.e., S-N curve) and $[A]$ and $[D]$ matrices of approximately 10,000 different laminates were computed and stored as the synthetic data. They were divided into training (80%), validation (10%), and test data (10%). It was also noticed that when training either the conventional MLP neural net or the RNN, training is much better for fatigue prediction when the data covers the full range of the fatigue curve (e.g., life between 1000 and $1E9$ cycles). To facilitate the use of the developed surrogate models for the prediction of the ABD matrices and the full range of the S-N curve a Python GUI was developed [29].

¹ Each ply of the laminate has the same thickness.

Table I. Data Generation: Input Parameter Ranges

Property	Upper	Lower
RUC/Laminate Properties		
FVR	0.4	0.7
Θ_1	-90	90
Θ_2	-90	90
Θ_3	-90	90
Θ_4	-90	90
Constituent Deformation Properties		
Fiber		
Efa, GPa	70	700
Eft, GPa	70	200
vfa	0.2	0.4
vfa	0.2	0.4
Gfa, GPa	25	200
Matrix		
Em, GPa	2.5	4.5
vm	0.2	0.45
Constituent Fatigue Parameters		
Fiber		
SU11, MPa	2500	9500
SU21, MPa	300	2500
Matrix		
Epsm1	0.015	0.03
Epsm2	0.015	0.03
β	4	12
SFL, MPa	15	30
XML, MPa	80	160

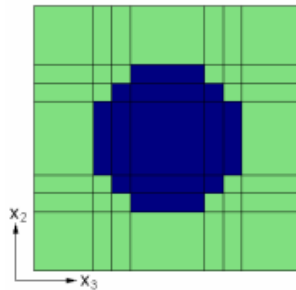


Figure 5. 7x7 RUC used for data generation

Table II. Implicit relationship between Fiber properties and Matrix properties.

Fiber properties: <ul style="list-style-type: none"> <input type="checkbox"/> $E_t \leq E_a$ <input type="checkbox"/> $E_t/(2(1+\nu_t)) \leq G_a \leq E_a/(2(1+\nu_a))$ <input type="checkbox"/> $SU_{12} = SU_{13} = (SU_{11}/E_a) * E_t$ <input type="checkbox"/> $SU_{14} = SU_{12}/\sqrt{3}$ <input type="checkbox"/> $SU_{15} = SU_{16} = SU_{11}/\sqrt{3}$ <input type="checkbox"/> $SU_{21} < SU_{11}$ <input type="checkbox"/> $SU_{22} = SU_{23} = (SU_{21}/E_a) * E_t$ <input type="checkbox"/> $SU_{24} = SU_{22}/\sqrt{3}$ <input type="checkbox"/> $SU_{25} = SU_{26} = SU_{21}/\sqrt{3}$ <input type="checkbox"/> $X_{11}=SU_{11}, X_{22}=SU_{12}, X_{33}=SU_{13}, X_{23}=SU_{14},$ $X_{12}=SU_{15} X_{13}=SU_{16}$ 	Matrix properties: <ul style="list-style-type: none"> <input type="checkbox"/> $S_u = E_m * \epsilon_{sm1}$ (failure is based on strain and is assumed linear until failure)
--	---

RESULTS

Two types of neural nets MLP and RNN were developed to predict the laminate stiffness and fatigue curves. Both types of networks provided results with excellent accuracy and speed.

Stiffness Prediction

A standard MLP neural net was trained to predict the stiffness (i.e., A and D matrices) for an eight-ply symmetric laminate (i.e., $B = 0$). There are 12 input parameters – four angles, five fiber elastic properties for a transversely isotropic fiber (axial and transvers modulus, axial and transverse Poisson's ratios, axial shear modulus) and two matrix elastic properties for an isotropic matrix (modulus, Poisson's ratio). There were 12 output properties – six components associated with the A matrix (3x3 symmetric matrix) and six components of the D matrix (also a 3x3 symmetric matrix). The specific neural net for stiffness prediction had five hidden layers and 26 nodes in each layer. The mean square error (MSE) for stiffness prediction was 0.02. Figure 6 shows the comparison between the ANN stiffness prediction of a random laminate, $[-17^\circ/35^\circ/-72^\circ/5^\circ]_s$, with that produced from MAC/GMC (labelled as actual in Fig. 6). Results show excellent agreement between the predicted and actual values. It should be noted that when the target values are relatively small (e.g., very close to zero), somewhat amplified errors can occur.

Prediction of Fatigue (S-N) Curve

Training of a neural net to predict the fatigue curve for a given laminate configuration turned out to be a much more complex process. The ANN for the fatigue life prediction has added complexity where the number of inputs increase from 12 to 19 as the inputs for fatigue related properties must be considered as well, see Table 1 and 2. The calculation of fatigue life is where the development of an ANN estimator shows its true benefit; as physics-based model prediction of fatigue life can take anywhere from minutes to hours to compute the entire S-N curve, depending upon the laminate specification. Consequently, all fatigue synthetic data (training data instances) were run on a Linux cluster.

	Predicted	Actual	% Error
A11	2.7824e+05	2.7839e+05	0.06
A12	55536	55654	0.21
A13	13624	13660	0.26
A22	1.3209e+05	1.3204e+05	-0.04
A23	-15535	-15488	-0.3
A33	50057	50008	-0.1
D11	1.0162e+05	1.0178e+05	0.16
D12	21948	21955	0.03
D13	-8392.7	-8378.8	-0.17
D22	28278	28220	-0.2
D23	673.36	707.9	4.88
D33	20118	20073	-0.22

Figure 6. Comparison of NN (predicted) and GMC (actual) output for a random laminate, $[-17^\circ/35^\circ/-72^\circ/5^\circ]_s$.

As mentioned before, two different types of neural nets were trained to predict the fatigue life of a given laminate as described below.

Multi-Layer Perceptron (MLP) Network

Also sometimes loosely referred to as simply an artificial neural network (ANN), MLP is the most common and the simplest form of a deep learning neural network. An ensemble deep learning neural net was employed. An ensemble approach is used to reduce the variance of neural network models by training multiple models instead of a single model and to combine the predictions from these models. This is called ensemble learning and it not only reduces the variance of predictions but also can result in predictions that are better than any single model. A schematic of an ensemble model is shown in Figure 7.

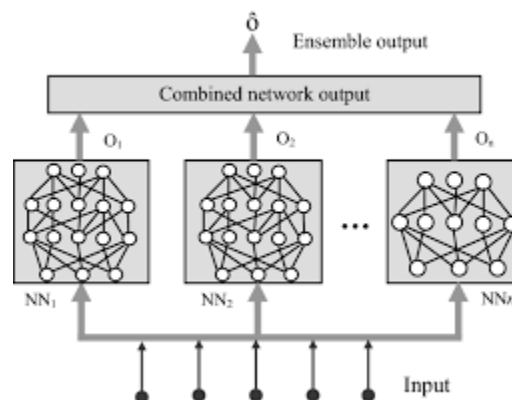


Figure 7. Deep learning ensemble neural net

Thirty sub-models or neural nets were trained to predict the log of fatigue life (Log N) that is expected to be between 3 and 9 given all the inputs for the laminate including the fatigue load. Each individual neural net (sub-model) consists of 6 hidden layers with 48 neurons in each layer. The mean square error (MSE) ranged from 0.25

to 0.32 for the 30 sub models. The output from these 30 sub models was then combined using a simple linear stacked model and the overall error (MSE) reduced to 0.104 with the mean absolute error (MAE) in Log N being 0.181.

The fatigue (S-N) curve for a laminate is defined by 10 points (Stress vs. Number of cycles to failure pairs). To obtain an S-N curve, the MLP model is called at each applied load to predict a single value of life. About 5000 laminates (50,000 rows of data) was used for training and validation while the test data consisted of approximately 600 laminates (6000 rows of data each). These laminates consisted of angles that were purely random as well as those with custom angles such as [0], [90], cross-ply [0/90], quasi-isotropic [0/±45/90], etc. Each laminate had a full range of stress values which provided number of cycles to failure ranging from approximately 1E3 to 1E9. Also, the training set consisted of 40% random and 60% custom laminates. When the trained neural net was tested on validation and test data, it showed that the:

Probability that a prediction will lie within $\pm 10\%$ log of target was 84.4%
Probability that a prediction will lie within $\pm 20\%$ log of target was 94.6%
Probability that a prediction will lie within $\pm 30\%$ log of target was 97.4%

Note that $\pm 10\%$ log (N) is approximately equivalent to $\pm 300\%$ of target N, which is within typical experimental error, which is in the range of 2x-4x.

Figure 8 shows the comparison between the neural net prediction of the fatigue curve (blue line) vs. the simulated (red line) curves using the physics-based model MAC/GMC, for 16 laminates with a mixture of custom and random laminates. It shows that the ANN predictions are a good estimate of the actual fatigue curves, with an MSE range of 0.01 to 1.27 for these 16 laminates. However, these predictions are made at a fraction of the cost (CPU time and effort) compared to the actual physics-based model (i.e., MAC/GMC); e.g., 1.8×10^{-04} . Note the worst error occurs for the random angled laminates.

Recurrent Neural Network (RNN)

As mentioned before, an RNN was also trained using the same virtual data set even though our model and data do not fit the traditional definition of RNN. However, given a specific laminate (volume fraction, ply angles, constituent material properties) MAC/GMC predicts the fatigue life (number of cycles to failure) for a given fatigue load, thus providing a series of implicitly related points (S vs. N) for a given laminate.

The RNN consisted of one dense and one LSTM (Long Short-Term Memory) layer with 20 neurons each, which was a relatively simple architecture. Unlike the MLP, the vector of applied loads is passed to the model **once** to predict the full S-N curve. The MSE for fatigue life prediction was 0.01 and MAE was 0.06 (for log N) for validation cases, which is remarkably better than what was achieved using an MLP network. The training/validation data that was used to develop the MLP was also used here. The results on validation cases showed that the:

Probability that a prediction will lie within $\pm 5\%$ log of target was 92%
Probability that a prediction will lie within $\pm 10\%$ log of target was 98%
Probability that a prediction will lie within $\pm 20\%$ log of target was 100%

Note that $\pm 5\%$ log (N) is approximately equivalent to $\pm 200\%$ of target N, which is well within the typical scatter range that is observed in experimental data; i.e., $2x-4x$.

The predicted and target S-N response curves for 16 cases randomly selected from the validation set are shown in Figure 9. Results indicate that the RNN predictions are a very good estimate of the actual fatigue curves, with an MSE range of 0.0 to 0.08 for these 16 laminates. Clearly, the RNN model provides overall significantly better results than what was observed using the MLP network (see Fig. 7).

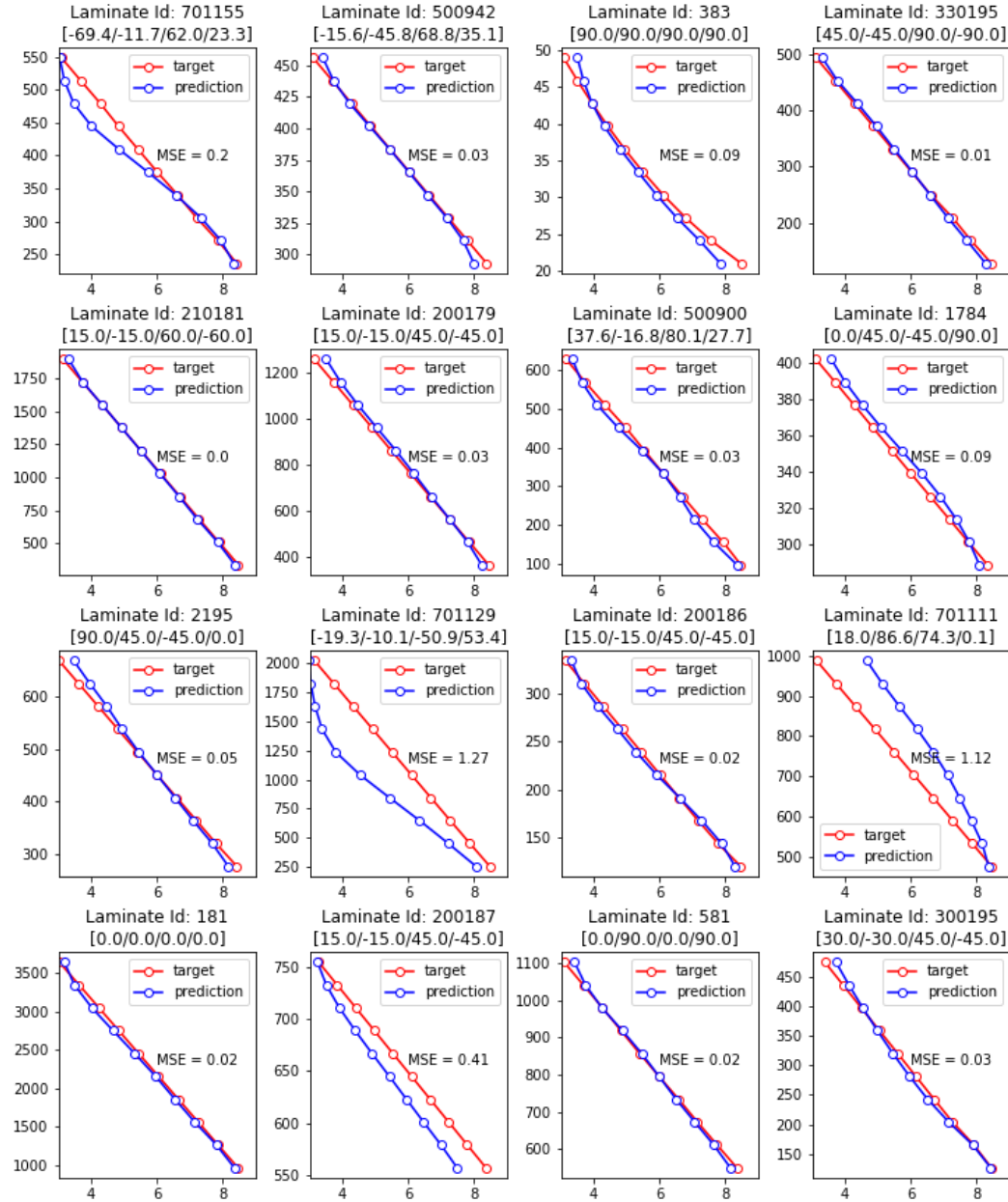


Figure 8. MLP Comparison of predicted and actual fatigue curves of few laminates

Note the results observed here are opposite to those observed in the case of MPL model where the random laminate predictions were substantially worse than the custom angled laminates. This prompted us to investigate the influence of the training data set mixture between custom and random angles. Table III shows the results of this

sensitivity study. Results show that overall accuracy improves when laminates with random angles are increased in the training set. As expected, the prediction of laminates with random angles improves significantly while laminates with custom angles degrades slightly. RNN model fatigue life predictions are in general better, as they are better able to capture the **shape** of the fatigue curve.

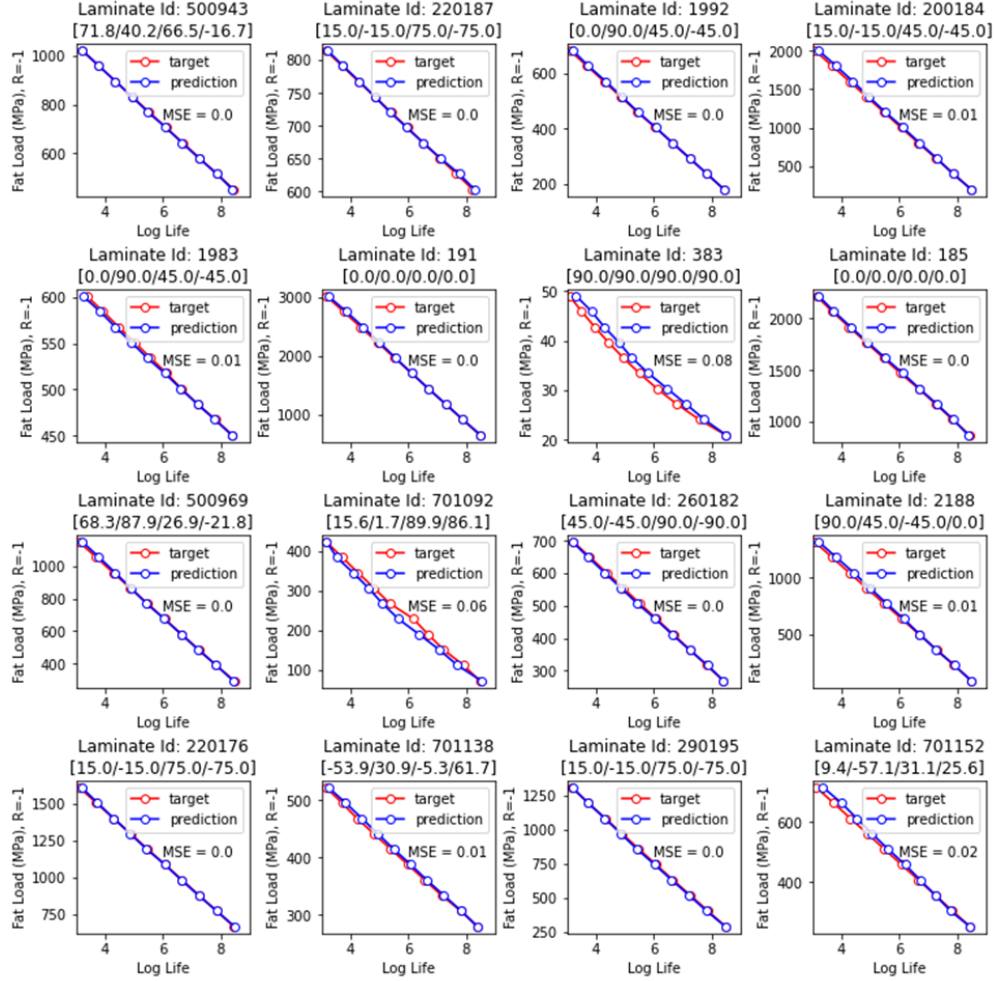


Figure 9. RNN Comparison of the Actual and Predicted S-N curves of Few Random Laminates.

Table III. MSE results given different mixture of data sets for total validation set (μ is mean and σ is standard deviation)

	Random (40%) & Custom (60%)		Random (60%) & Custom (40%)	
	MLP	RNN	MLP	RNN
Total	$\mu = 0.26$ $\sigma = 0.93$	$\mu = 0.04$ $\sigma = 0.22$	$\mu = 0.07$ $\sigma = 0.18$	$\mu = 0.003$ $\sigma = 0.12$
Random	$\mu = 0.59$ $\sigma = 1.48$	$\mu = 0.05$ $\sigma = 0.3$	$\mu = 0.03$ $\sigma = 0.17$	$\mu = 0.001$ $\sigma = 0.04$
Custom	$\mu = 0.08$ $\sigma = 0.19$	$\mu = 0.03$ $\sigma = 0.13$	$\mu = 0.12$ $\sigma = 0.19$	$\mu = 0.04$ $\sigma = 0.18$

CONCLUSIONS

ANN models using both MLP and RNN were developed to predict micromechanics-based laminate stiffnesses (ABD) and fatigue life of eight-ply, symmetric, PMC laminates. Deep learning artificial neural nets require a large amount of data for training/validation to achieve a certain level of accuracy. Generally, that amount of experimentally measured data is not available because of the cost and time involved. Therefore, synthetic/virtual data was generated using the physics-based MAC/GMC micromechanics model. The 10,000 laminates simulated required approximately 15,000 hours of computations. Results indicate that the ANN based model can indeed accurately predict the laminate stiffness (i.e., ABD matrix) and fatigue life response of PMC laminates at a fraction of the cost (CPU time) compared to the actual physics-based model. Models based on both ANN (MLP) and RNN were able to predict the stiffness quite accurately, but in general the RNN model was better able to capture the character of the fatigue curve with generally better accuracy and less computational time. As such, an ML stiffness and fatigue life estimator tool was developed which designers can use for system level studies to obtain an estimate of desired properties and life of 8-ply symmetric PMC composite laminates with significantly less resources (CPU time, user effort and training). For example, given the generation of an entire typical S-N curve took approximately 1.5 hours for MAC/GMC and the surrogate was approx. 1 sec, this amounts to a speed up of 1.8×10^{-4} . Similarly, the ply level Neural Net based surrogate models can be used in composite multiscale analyses to replace the actual physics-based calculations at lower scales and thereby significantly reduce the computational times of such analyses. These models thus enable multiscale analyses spanning several levels as viable industrial tools.

ACKNOWLEDGMENT

Primary development was funded through the NASA Aeronautics Research Mission Directorate's (ARMD's) Transformational Tools and Technologies (TTT) Project. Thanks also to Josh Stuckner, Multiscale and Multiphysics branch of NASA Glenn Research Center for many helpful discussions.

REFERENCES

1. Brynjolfsson, Erik and Mitchell, Tom, "What Can Machine Learning Do? Workforce Implications", Science, Vol. 358, No. 6370, 2017. DOI: [10.1126/science.aap8062](https://doi.org/10.1126/science.aap8062)
2. Jackson, P., Introduction to Expert Systems, 3rd ed., Addison-Wesley, 1999.
3. Marsland, S. Machine Learning. CRC Press, Taylor & Francis Inc., Boca Raton, FL, 2014.
4. Haykins, S. Neural Networks. Prentice-Hall, 1999.
5. Wong, T.T., "Advances in ICME Implementations: Concepts and Practices, JOM Vol. 69, No. 879, 2017.
6. Arnold, S.M., Holland, F.A., Bednarczyk, B.A., Pineda, E.J., "Combining Material and Model Pedigree is Foundational to making ICME a Reality", Integrating Materials and Manufacturing Innovation, 4, 2015. DOI:10.1186/s40192-015-0031-2.
7. Liu, X., Tian, S., Tao, F., Yu, w., "A Review of Artificial Neural Networks in the Constitutive Modeling of Composite Materials", Composite Part B: Engineering, Vol. 224, Nov. 2021. <https://doi.org/10.1016/j.compositesb.2021.109152>.

8. Arnold, S.M., Piekenbrock, M., Ricks, T.M., Stuckner, J., “Multiscale Analysis of Composites Using Surrogate Modeling and Information Optimal Designs”, Proc. 2020 AII SciTech Conference, Orlando, FL, Jan. 6-10, 2020. DOI:10.2514/6.2020-1863.
9. Stuckner, J., Graeber, S., Weborg, B., Ricks, T. M., & Arnold, S. M. (2021). Tractable Multiscale Modeling with An Embedded Microscale Surrogate. In AIAA SciTech 2021 Forum, DOI: 10.2514/6.2021-1963.
10. Bednarczyk, B. A., and Arnold, S. M.; “MAC/GMC 4.0 User’s Manual, Volume 2: Keywords Manual”, TM 2002-212077/Vol 2, 2002.
11. Aboudi, J., Arnold, S.M., and Bednarczyk, B.A.; *Micromechanics of Composite Materials: A Generalized Multiscale Analysis Approach*, Elsevier, Inc., 2013.
12. Aboudi, J., Arnold, S.M., and Bednarczyk, B.A., (2021); *Practical Micromechanics of Composite Materials*, Elsevier, Butterworth-Heinemann, 2021.
13. Paley, M. and Aboudi, J., (1992) “Micromechanical Analysis of Composites by the Generalized Cells Model” *Mechanics of Materials*, 14:127–139.
14. Aboudi, J., Pindera, M.J. and Arnold, S.M.; “Higher-Order Theory for Periodic Multiphase Materials with Inelastic Phases”, NASA/TM 2002-211469. Also see IJP, 2003, 19: 805-847.
15. Romanov, V., Lomov, S. V., Swolfs, Y., Orlova, S., Gorbatiikh, L., and Verpoest, I. (2013). Statistical Analysis of Real and Simulated Fibre Arrangements in Unidirectional Composites. *Composites Science and Technology*, 87:126-134.
16. Garnich, M. R., Fertig, R. S., and Anderson, E.M.; “Random Fiber Micromechanics of Fatigue Damage”, 54th AIAA/ASME/ASCE/AHS/SC Structures, Structural Dynamics, and Materials Conference, AIAA 2013-165, Boston, MA, April 8-11, 2013.
17. N. E. Dowling, *Mechanical Behavior of Materials: Engineering Methods for Deformation, Fracture, and Fatigue*, Prentice Hall, New Jersey. 1999.
18. J. Lemaitre and Chaboche, J.L., *Mechanics of Solid Materials*, Cambridge University Press, 1990.
19. Skrzypek, J. and Hetnarski, R. *Plasticity and Creep Theory Examples and Problems*. Boca Raton, FL.: CRC Press, 1993.
20. Arnold, S. M. and Kruch, S., “A Differential CDM Model For Fatigue of Unidirectional Metal Matrix Composites”, *Int. Journal of Damage Mechanics*, Vol. 3, No. 2, pp.170-191
21. Chaboche, J.L. and Lesne, P.M.; “A Non-Linear Continuous Fatigue Damage Model”, *Fatigue Fract. Engn. Mater. Struct.*, 11(1): 1-7., 1988.
22. Wilt, T.E., Arnold, S.M., and Saleeb, A.F.; “A Coupled/Uncoupled Computational Scheme for Deformation and Fatigue Damage Analysis of Unidirectional Metal-Matrix Composites”, *Applications of Continuum Damage Mechanics to Fatigue and Fracture*, ASTM STP 1315, D.L. McDowell (Ed.), 65-82, 1997.
23. Bednarczyk, B. A., and Arnold, S. M.; “MAC/GMC 4.0 User’s Manual, Volume 3: Example Problem Manual”, TM 2002-212077/Vol 3, 2002.
24. Kruch, S. and Arnold, S. M., “Creep Damage and Creep-Fatigue Damage Interaction for Metal Matrix Composites “Applications of Continuum Damage Mechanics to Fatigue and Fracture, ASTM STP 1351, D.L. McDowell, Ed., American Society for Testing and Materials, pp. 7-28.
25. Chollet, Francois, *Deep Learning with Python*. Manning Publications Co, New York. 2018.
26. Paluszek, M., Thomas, S., Ham, E., *Practical MATLAB Deep Learning – A Projects-Based Approach*, 222nd ed., Apress, 2022.
27. *Anaconda Python for Windows version 3.9*, 2022.
28. Hearley, B., Arnold, S.M., Stuckner, J.; *A Robust Machine Learning Schema for Developing, Maintaining, and Disseminating Machine Learning Models*, NASA/TM-20220017137, 2022.
29. Mital, S.K. Arnold, S.M., Murthy, P.L.N., Hearley, B.L.: *Prediction of Stiffness and Fatigue Lives of Polymer Matrix Composite Laminates Using Artificial Neural Networks*, NASA/TM-20230005410, May 2023.